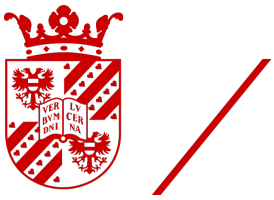

university of groningen

Stability of Group Self-Annuitization Funds under Inflation

Paolo Conorto
S4681576

June 16, 2025

Bachelor's Thesis Econometrics and Operations Research

Supervisor: dr. K.W. Chau

Second assessor: dr. W. Zhu

university of groningen

Stability of Group Self-Annuitization Funds under Inflation

Paolo Conorto

Abstract

Group Self-Annuitization (GSA) schemes offer a decentralized alternative to traditional life annuities by pooling longevity and investment risks among retirees. This thesis investigates whether GSA pools can maintain stable real income under inflationary pressure in a Dutch context. A dynamic simulation framework is developed, incorporating stochastic forecasts of inflation and interest rates via a Vector Error Correction Model (VECM) with GARCH-based residuals. Monte Carlo simulations are conducted across varying pool sizes, asset allocations, and payout strategies, including backloaded schemes.

Findings show that while large pool sizes enhance nominal stability, they fail to preserve purchasing power when returns lag behind inflation. Modest equity allocations (e.g., 20%) extend real income sustainability but remain insufficient alone. Introducing a deferred payout structure in combination with equity exposure significantly improves real stability and actuarial fairness. These results suggest that preserving real income in GSAs requires a careful balance between payout timing and exposure to growth assets.

Contents

1 Introduction

With life expectancy continuing to rise globally, retirement products are necessary to ensure that retirees can maintain financial stability. It is common for retirees to finance their retirement through insurance companies, pension funds or banks, which convert savings into a steady cash flow. This is observed in countries with a long history of reliable retirement plans, as well as in those with robust public pension systems. However, as providers refrain from offering full payout guarantees (Hieber and Lucas, 2022), demand emerges for new products. Retirees may resort to using personal savings during retirement or purchasing classic insurance products privately. The latter is a riskier alternative due to the uncertainty of outliving one's funds, while the former tends to be underutilized by the general population. For example, despite their availability, only about 6% of Dutch pensions are attributed to private purchases, indicating limited engagement with individual private pension plans Knoef et al. (2023).

To address these challenges, we propose circumventing traditional intermediaries and adopting Group Self-Annuitization (GSA) funds. GSAs offer an alternative amid an aging population, currently with providers struggling to guarantee payouts and the shift from defined benefit to defined contribution schemes. A GSA is a financial agreement among a group of individuals who contribute their savings to a common pool and receive regular payments from the combined fund over time until their death. Upon a member's death, their share is redistributed among the surviving participants, thereby reducing the risk of outliving one's cash flows. This arrangement is typically executed without an intermediary, ensuring that all contributions are directed towards payouts and avoiding commissions. However, this also implies reliance on non-professional portfolio management and the possibility of suboptimal returns (Otuteye and Siddiquee, 2019). Moreover, the fund's success is highly dependent on the number of participants and may under-perform with small pools.

Given the relatively low annual returns characteristic of risk-free rate investment strategies, it is evident that even with the full depletion of the GSAs fund, real purchasing power may not be preserved. This study examines the challenges GSAs face in maintaining purchasing power under projected inflationary scenarios, time-varying interest rates, and conventional equity return assumptions. We model financial returns and inflation as forecasted time series using Auto-Regressive Moving Average (ARMA) and Vector Error Correction Model (VECM) frameworks, specifying residuals to follow a Generalized Auto-Regressive Conditional Heteroskedasticity (GARCH) process with Student's t-distributions to account for the possibility of fat-tailed behavior in financial data.

To assess real cash flow stability, we simulate fund dynamics under these forecasts until either the fund's collapse or the death of all members. Nominal returns are derived from interest rate projections within the VECM, while real income is adjusted using forecasted inflation. Fund stability is evaluated by measuring the percentage of real cash flows that remain above an arbitrary lower bound until a specified arbitrary time. We further test the inclusion of riskier securities in the portfolio to analyze their impact on real-income sustainability by forecasting their yearly returns. Finally, we propose a modified GSA payout structure with inflation-indexing mechanisms and discuss its implications for maintaining stable real payouts. Our central research question is: *Can Group Self-Annuitization funds remain stable under inflationary erosion?* We contribute to the literature by modeling inflationary risks in GSAs through stochastic forecasting models and proposing a mechanism to enhance real payout stability without the inclusion of complex investment strategies. To our knowledge, this is the first analysis to integrate GARCH-based inflation and interest rate projections into GSA sustainability assessments.

2 Literature Review

The literature surrounding Group Self-Annuitization (GSA) funds is comprehensive and has evolved significantly in recent decades. Piggott et al. (2005) introduced the foundational framework for GSAs, proposing a pooled structure that enables individuals to collectively share longevity risk by contributing their retirement savings into a communal fund. Within this arrangement, systematic mortality risk is individually borne, whereas idiosyncratic mortality risk is shared among participants. Each

member's annual income stream is derived based on their individual portfolio value and an annuity factor calculated using assumed survival probabilities. This method guarantees lifelong payouts, provided that actual survival probabilities and investment returns align with expectations. Such design helps stabilize incomes over an individual's retirement period, mitigating the volatility associated with longevity risk by redistributing benefits from deceased members to survivors.

Extending this foundational work, Stamos (2008) demonstrated the significant utility enhancement offered by pooled annuity funds, reinforcing the fact that more constituents imply greater mortality credit distribution. Optimal consumption rates in his analysis grew with participant numbers and age, reinforcing the social benefits of pooling, particularly among populations with greater heterogeinity in mortality risks. Similarly Valdez et al. (2006) confirmed Stamos's findings whilst delving deeper into investigating market dynamics and consumer behaviors impacting demand for pooled versus conventional annuities.

Furthermore, within the refined conceptual framework, Bernhardt and Donnelly (2021) provided an analytical exploration of the trade-offs between income stability and participant count. They highlighted how achieving stable payouts requires sufficiently large member pools to diversify unsystematic mortality risk effectively. Their findings underscore a critical constraint in GSA design: the necessity of balancing member count against fund volatility, particularly under assumptions of homogeneity across participants in terms of portfolio value and survival expectations.

Moreover, Bernhardt and Qu (2024) emphasized the destabilizing effects introduced by substantial variations in initial portfolio values, with wealthier participants amplifying income volatility within pooled funds. They found a clear threshold where income disparities became pronounced enough to prompt less affluent individuals to seek alternative pooling arrangements excluding significantly wealthier counterparts.

Expanding upon optimal payout strategies, Milevsky and Salisbury (2015) examined tontines, a product closely related to pooled annuity funds, and demonstrated optimal payout structures involving declining payouts over time. Similarly, Li et al. (2022) explored integrating equity investments with managed-volatility strategies within pooled annuity contexts. Their approach indicated significant improvements in fund performance, notably reducing downside risk and stabilizing income streams, the effect on real income is yet to be investigated.

With the purpose of concentrating on the effect of inflation, we shift our focus to its forecasting. Faust and Wright (2013) highlight the under-performance of Philips' curves in predicting inflation rates, underscoring the limitations of traditional macroeconomic models in the short to medium term. Therefore, we draw on dynamic econometric techniques, as demonstrated by Cross and Poon (2016), who employ VAR models with thick-tailed errors to achieve superior medium- to long-term forecasts for the Australian economy.

In their study, Cross and Poon (2016) investigate whether incorporating time variation and fat-tails into a suite of popular univariate and multivariate Gaussian distributed models improves forecasting performance. They find that models accounting for fat-tailed distributions provide better predictive accuracy for macroeconomic variables, including inflation and interest rates, particularly during periods of structural change. This suggests that accommodating non-Gaussian features in econometric models can enhance the reliability of macroeconomic forecasts. We therefore build on their findings in our macroeconomic modeling.

This thesis aligns with and builds upon these critical contributions, adopting structural elements from Piggott et al. (2005) and integrating contemporary approaches to systematically assess income stability within GSAs. Specifically, the research herein extends existing methodologies by explicitly incorporating the different payout structures and assessing the effect on maintenance purchasing power.

3 Model Formulation

This model is based on the Group Self-Annuitization (GSA) framework introduced by Piggott et al. (2005), which aims to provide longevity insurance without requiring guarantees from insurers or governments. It is assumed that the population is homogeneous with respect to demographics and mor-

tality, that is: all members follow the same mortality distribution based on the probabilities inferred from the Dutch mortality tables in Human Mortality Database (2023). Moreover, all members are the same age on the initial day of Fund inception (that is the first day of the year of inception, also implying that all birthdays are on the first day of each year) and the Fund is closed. Consistent with the approach outlined by Piggott et al. (2005), the fund is composed by a fixed group of n members, with $n \in \mathbb{N}$ and tracked in discrete time where $t \in \mathbb{N}$. The assumption of homogeneity, although highly restrictive, is substantiated by the fact that the product modeling in this case is for a very specific Dutch demographic in cases where the demographic likely heterogeneous cash flows can no longer be calculated fairly without prior knowledge of difference in mortality expectation. Hence, it follows that all n members become fund participants at time $t = 0$; no additional members are admitted once the fund is initiated. Consequently, any increase in the conjunct portfolio value at $t > 0$, shall be attributed to investment returns which will be defined later. The combined pool of funds shall be tracked by the Nominal Complete Portfolio Value Function $V_N(t) : \mathbb{N} \to \mathbb{R}^+$ as-well as the Real Complete Portfolio value Function $V_R(t) : \mathbb{N} \to \mathbb{R}^+$ these two always satisfy: $V_R(0) = V_N(0)$ and

$$V_R(t) = \frac{V_N(t)}{I_t}, \tag{3.1}$$

where the inflation index I_t is given by

$$I_t = \frac{CPI_t}{CPI_0}. \tag{3.2}$$

Where $\{CPI_t, t \in \mathbb{Z}\}$ represents the real value for the average Consumer Price Index (CPI) of the Netherlands obtained from the either the historical time series extracted from Organization for Economic Co-operation and Development (2025) or forecasted value. In which case CPI_t is chosen as the forecasted value for all $t > 0$ and the historical value is $\mathcal{H}_{CPI} = \{CPI_t, t \leq 0\}$. The CPI is forecasted in conjuction with the interest rate $\{r_t, t \in \mathbb{Z}\}$ which itself follows the one-year return of the 10-year Dutch government bonds De Nederlandsche Bank (2025) with $t > 0$ also representing forecasted values and $\mathcal{H}_r = \{r_t, t \leq 0\}$ - both data series follow monthly information but are only observed in the model at the beginning of the first day of the year. In this formulation, $t = 0$ corresponds to the most recently observed value in either series. For calculations that require discounting in an actuarial context, the actuarial discount rate is taken as the historical average of the interest rate time series: $r = \frac{1}{|\mathcal{H}_r|} \sum_{i \in \mathcal{H}_r} r_i$. The intuition behind the simplicity in modeling the actuarial discount rate arises from the nature of the GSA as a product; the GSA itself attempts to circumvent the costs an insurance company intakes. The GSA therefore does not follow traditional complex actuarial discount rate models because of the complicated nature in implementation into this simplified model.

3.1 Fund Members' Survival

At time $t = 0$, all n members have just turned age $x = 67$, which is the Dutch retirement age at which individuals become eligible for remuneration from the First-Pillar. We define the future lifetime of member i by the non-negative random variable T_i, where $T_i \geq 0$ for $i = 1, \ldots, n$. Each T_i is defined on a probability space $(\Omega, \mathcal{F}, \mathbb{P})$ and takes values in $\mathbb{R}^+$. The random variables $T_1, \ldots, T_n$ are assumed to be independent and identically distributed (i.i.d.). Moreover, the age at death for each member is then given by

$$K_x^{(i)} = \lfloor T_i \rfloor + x,$$

$K_x^{(i)}$ is treated as a discrete random variable taking integer values, representing the member's age at death. At the end of each discrete time period (or year), the number of surviving members is given by

$$L_{x+t} = \sum_{i=1}^{n} \mathbb{I}\{T_i > t\}, \quad \text{for } t \geq 0, \tag{3.3}$$

where $\mathbb{I}\{T_i > t\}$ is an indicator function equal to 1 if member i is alive at time t and 0 otherwise. The survival probability from age $x + t$ to age $x + t + 1$ is defined by

$$p_{x+t} = \mathbb{P}(T_i > t), \tag{3.4}$$

for every $t \geq 0$. Given the i.i.d. assumption, the individual indicators $\mathbb{I}\{T_i > t\}$ behave as Bernoulli random variables. Consequently, conditional on the number of survivors L_{x+t-1} at the previous time period, the number of survivors at time t is binomially distributed:

$$L_{x+t} \sim \text{Bin}\big(L_{x+t-1},\, p_{x+t-1}\big). \tag{3.5}$$

Furthermore, an empirical estimate of the survival probability at time t is given by

$$\hat{p}_{x+t} = \frac{L_{x+t+1}}{L_{x+t}}. \tag{3.6}$$

In practice, simulation realizations of $T_i \sim T_{\text{lifetable}}$ are taken using the observed Dutch mortality tables, with the process initiated at $L_x = n$, for $x = 67$. Both equations (3.5) and (3.6) then contribute to a rigorous assessment of the portfolio stability through the lifetime of each member.

3.2 Payment Streams

Next, we consider the nominal income received by each member until their respective age of death K_i. Since the group is homogeneous, it is assumed that the initial nominal account value defined for each member i by the function $v_i^N : \mathbb{N} \to \mathbb{R}^+$ where $v_i^N(0)$ is positive and equal for all i, i.e., $v_i^N(0) \geq 0$ for every $i = 1, \ldots, n$. Following the model setup outlined in Piggott et al. (2005), the nominal cashflow received by member i who is alive at time t is expressed as

$$\mathbb{I}\{T_i > t\} \frac{v_i^N(t)}{\ddot{a}_{x+t}}, \tag{3.7}$$

where the annuity-due factor $\ddot{a}_{x+t}$ is defined as the sum of discounted survival probabilities:

$$\ddot{a}_{x+t} = \sum_{j=0}^{\infty} \frac{1}{(1+r)^j}\, {}_jp_{x+t}. \tag{3.8}$$

In the above, ${}_jp_{x+t}$ denotes the probability that an individual aged $x+t$ will survive for an additional j years, that is:

$${}_jp_{x+t} = \mathbb{P}(T_i > t + j),$$

and the annuity discount rate follows from the historical mean as previously stated. However, with the addition of inflation and the centering of this study being specifically on real-income we deem that it is paramount to describe our cash flows as dependent on a loading function $f : \mathbb{R}^+ \times \mathbb{R}^+ \cup (-1, 0) \times \mathbb{N} \to \mathbb{R}^+$ that when not equal to 1 modifies the cash-flow's volume dependent on t:

$$B_i(t) = \mathbb{I}\{T_i > t\} \frac{v_i^N(t)}{\ddot{a}_{x+t}} f(\alpha, \beta, t), \tag{3.9}$$

with the loading function being:

$$f(\alpha, \beta, t) = g(t) \frac{\alpha}{1 + \beta^t}. \tag{3.10}$$

Where $g : \mathbb{N} \to \{0, 1\}$ is some arbitrary indicator function used to activate or deactivate loading in cash flows dependent on time.

3.3 Longevity Credit

When a member passes away, the remaining nominal portfolio value in their account, denoted by $v_i^N(T_i + 1)$, is redistributed equally among the surviving members. This reallocation, referred to as the longevity credit, is integrated into the overall portfolio dynamics. The complete portfolio remains invested in the 10-year bonds Dutch government bonds and the yearly returns of the Dutch Stock Market index (AEX) are represented as $\{AEX_t, t \in \mathbb{Z}\}$ where AEX_t follows the AEX price real time series and follows forecasted values for $t > 0$. Under the assumption that the bond return is free from

uncertainty (apart from liquidity shocks) and the AEX returns are regarded as given, the portfolio evolves nominally as

$$V_N(t) = \left(V_N(t-1) - L_{x+t-1}\, B_i(t-1)\right)(1+R_t), \tag{3.11}$$

where the portfolio return R_t is modeled according to

$$R_t = \mu\left(r_{t-1}^{AEX}\right) + (1-\mu)\left(r_{t-1} + \epsilon_t^p\right), \quad \epsilon_t^p \sim \mathcal{N}(0, \sigma_p^2). \tag{3.12}$$

Here, ϵ_t^p captures an idiosyncratic shock due to potential liquidity constraints when trading the bonds prior to maturity, $\mu \in [0,1]$ is the weight allocation of the portfolio. With this return, then nominal account value (disregarding longevity credits) is:

$$v_i^N(t)(1+R_t) - B_i(t). \tag{3.13}$$

And because for every time period $(t, t+1]$, the number of deaths is $(L_{x+t} - L_{x+t+1})$, and the total remaining nominal account value corresponding to the deceased members is redistributed equally among survivors immediately after applying returns, the longevity credit awarded to each surviving member at time $t+1$ is defined as:

$$\lambda(t+1) = \frac{(L_{x+t} - L_{x+t+1})\left(v_i^N(t) - B_i(t)\right)(1+R_t)}{L_{x+t+1}}. \tag{3.14}$$

Consequently, the nominal portfolio value of each surviving member at time $t+1$ is updated according to:

$$v_i^N(t+1) = \left[\left(v_i^N(t) - B_i(t)\right)(1+R_t) + \lambda(t+1)\right]\mathbb{I}\{T_i > t+1\}. \tag{3.15}$$

This formulation explicitly incorporates the redistribution mechanism inherent in the GSA fund into each individual's account dynamics, ensuring immediate redistribution of longevity credits from deceased members at the beginning of each year. Importantly, the longevity credit awarded at the start of period $t+1$ does not affect the payment $B_i(t)$ made during period t.

3.4 Interest Rate, Inflation and Stock Returns

Given that the objective of this study is to analyze the stability of the real income generated by the portfolio, it is necessary to provide explicit definitions for the variables driving inflation interest rates and stock returns. The inflation index, CPI_t, is based on a forecast of the actual CPI in the Netherlands dating back to 1960. Meanwhile, the interest rate r_t is derived from the observed one-year return on Dutch 10-year bonds, with data available on a monthly basis since 2001, the choice in the maturity comes from the higher historical returns 'healthy' yield-to-maturity ratios entail following Hautsch, Nikolaus and Ou, Yangguoyi (2008) rationale. These monthly time series are forecasted using a Vector Error Correction (VECM) model augmented by Generalized Autoregressive Conditional Heteroskedacity (GARCH) residuals with thick-tailed residuals.

For times $t < 0$, the model employs historical data for CPI_t and r_t. At time $t = 0$, the values CPI_0 and r_0 are set as the last common available data points from both series, marking the inception of the GSA fund. Note however, that although t has been a yearly time variable throughout the GSA for the nature forecast it follows monthly to increase the number of available data point in the historical series. For $t > 0$, forecasts for both series are generated with $\pi_t = CPI_t - CPI_{t-1}$ by the forecast of the following VECM model:

$$\Delta\begin{bmatrix}\pi_t \\ r_t\end{bmatrix} = \mathbf{b_t} + \begin{bmatrix}\alpha_1 \\ \alpha_2\end{bmatrix}\begin{bmatrix}\beta_1 & \beta_2\end{bmatrix}\begin{bmatrix}\pi_{t-1} \\ r_{t-1}\end{bmatrix} + \sum_{i=1}^{p-1}\begin{bmatrix}\gamma_{11}^{(i)} & \gamma_{12}^{(i)} \\ \gamma_{21}^{(i)} & \gamma_{22}^{(i)}\end{bmatrix}\Delta\begin{bmatrix}\pi_{t-i} \\ r_{t-i}\end{bmatrix} + \begin{bmatrix}\epsilon_t^I \\ \epsilon_t^r\end{bmatrix}. \tag{3.16}$$

In (3.16), $\mathbf{b_t}$ is a two-dimensional vector of intercepts, α is a 2×1 vector of adjustment coefficients capturing the rate at which deviations from the long-run equilibrium are corrected, and β is a 2×1 cointegration vector defining the long-run equilibrium relationship between the variables. The matrices:

$$\Gamma_i = \begin{bmatrix}\gamma_{11}^{(i)} & \gamma_{12}^{(i)} \\ \gamma_{21}^{(i)} & \gamma_{22}^{(i)}\end{bmatrix},$$

collect the short-run dynamic coefficients associated with lagged differences of the variables. The error terms ϵ_t^I and ϵ_t^r are modeled by a thick-tailed GARCH process:

$$\epsilon_t^I = \sigma_t^I \, Z_t^I, \quad Z_t^I \sim t_{v_I}(0,1), \tag{3.17}$$

$$\epsilon_t^r = \sigma_t^r \, Z_t^r, \quad Z_t^r \sim t_{v_r}(0,1), \tag{3.18}$$

with conditional variances specified as

$$(\sigma_t^I)^2 = \alpha_0 + \sum_{j=1}^{q} \alpha_j \left(\epsilon_{t-j}^I\right)^2 + \sum_{k=1}^{p} \gamma_k (\sigma_{t-k}^I)^2, \tag{3.19}$$

$$(\sigma_t^r)^2 = \alpha_0 + \sum_{j=1}^{u} \beta_j \left(\epsilon_{t-j}^r\right)^2 + \sum_{k=1}^{v} \delta_k (\sigma_{t-k}^r)^2. \tag{3.20}$$

Cross and Poon (2016) use of a VAR model with GARCH-t residuals for medium term forecasts of the equivalent Australian time series indicating that inflation and interest rates are strongly correlated, primarily due to monetary policies that simultaneously affect both variables. The VECM formulation of the combined times series is implemented in our forecast instead because of the Co-integration the series exhibit; relation backed by the real world relation Central banks have when manipulating interest rates in the pursuit of change is macoreconomical variables like inflation. The t-GARCH residuals are important in capturing variance clustering and tail events (for example, recessions or booms) which are often underestimated by models assuming normally distributed residuals.

3.4.1 Stock Returns

The Dutch equity return series $r_t^{AEX} = AEX_t - AEX_{t-1}$ is modeled independently of inflation and interest-rate processes to maintain a constant link between nominal and real portfolio returns across different equity allocations μ. We adopt a parsimonious ARMA–t-GARCH specification, which balances empirical realism with ease of integration into the GSA return structure framework.

Formally, the return process is given by

$$r_t^{AEX} = \mu_{AEX} + \sum_{i=1}^{p} \phi_i \, r_{t-i}^{AEX} + \sum_{j=1}^{q} \theta_j \, \epsilon_{t-j}^{AEX} + \epsilon_t^{AEX}, \tag{3.21}$$

with innovations and volatility dynamics

$$\epsilon_t^{AEX} = \sigma_t^{AEX} \, Z_t^{AEX}, \qquad Z_t^{AEX} \sim t_\nu(0,1), \tag{3.22}$$

$$(\sigma_t^{AEX})^2 = \alpha_0 + \sum_{k=1}^{r} \alpha_k \left(\epsilon_{t-k}^{AEX}\right)^2 + \sum_{\ell=1}^{s} \gamma_\ell \left(\sigma_{t-\ell}^{AEX}\right)^2. \tag{3.23}$$

This ARMA–t-GARCH approach builds on the foundational time-series modeling of Box and Jenkins for ARMA processes Box and Jenkins (1976), the introduction of ARCH by Engle (1982) and its extension to GARCH by Bollerslev Bollerslev (1986). The simplicity of this specification makes it straightforward to incorporate a stock component into the GSA without adding undue complexity in the interest rate and inflationary forecasts.

3.5 Stability of the GSA

The ultimate objective of the GSA fund is to provide a stable income stream that preserves the purchasing power of the beneficiaries. Although the nominal income, $B_i(t)$, may be stable in absolute terms, its real value could be eroded by inflation. Accordingly, we define the real income received by each member as:

$$B_i^R(t) = \frac{B_i(t)}{I_t}. \tag{3.24}$$

Stability in the nominal payment is ensured by requiring that the cashflow at any time t remains within a specified tolerance band around the initial cashflow, that is,

$$B_i(t) \in \Big[(1-\varepsilon_1)B_i(0),\ (1+\varepsilon_2)B_i(0)\Big], \tag{3.25}$$

where ε_1 and ε_2 are predetermined tolerance levels. Because the nominal cashflow is adjusted by the inflation index to obtain the real cashflow, the corresponding condition for real income is written as

$$B_i^R(t) \in \Big[(1-\varepsilon_1^R)B_i(0),\ (1+\varepsilon_2^R)B_i(0)\Big], \tag{3.26}$$

with $(1-\varepsilon_1^R)B_i(0)$ and $(1+\varepsilon_2^R)B_i(0)$ representing the lower and upper thresholds for acceptable real income fluctuations, respectively.

In addition to these period-by-period constraints, it is interesting to verify that the initial investment into the GSA fund retains its real value over time. This is assessed by comparing the cumulative real cash flows with the initial investment, this requirement is expressed as

$$\sum_{t=0}^{K_x^{(i)}-x} B_i^R(t) \in \Big[(1-\varepsilon_1^P)v_i(0),\ (1+\varepsilon_2^P)v_i(0)\Big], \tag{3.27}$$

where ε_1^P and ε_2^P are tolerances that define the acceptable deviation of the cumulative, real disbursed value from the initial investment. This condition ensures that, over the lifetime of a member, the total real benefits received remain actuarily fair in expectation.

4 Simulation Design and Parameter Calibration

4.1 Data

As outlined previously, the GSA model is calibrated within a Dutch context. Consequently, the mortality component is based on survival probabilities p_{x+t} obtained from Dutch cohort life tables, as published by Human Mortality Database (2023). These tables provide annual survival probabilities for cohorts aged 0 to 109, with $p_{110} = 0$ imposed to reflect the negligible probability of survival beyond age 110.

The historical time series of nominal interest rates $\{r_t\}_{t\in\mathbb{Z}}$ is sourced from De Nederlandsche Bank (2025), specifically using the yields of 10-year Dutch sovereign bonds to represent long-term risk-free rates.

CPI data for the Netherlands is obtained from the Federal Reserve Bank of St. Louis (FRED) database Organization for Economic Co-operation and Development (2025), providing a comprehensive historical monthly series dating back to the 1960s.

Lastly, historical prices for the AEX index are retrieved through an API interfacing with *investing.com*, covering daily closing values from 2001 onward. This dataset serves as the primary proxy for Dutch equity market performance.

4.2 Forecast Model Specification

To assess the long-run equilibrium relationship between inflation and interest rates, we employ a VECM without a deterministic trend component. This specification is appropriate given that both the monthly inflation rate π_t and the nominal interest rate r_t oscillate around a stable mean over time, despite the non-stationary nature of their levels (e.g., CPI_t), which display persistent growth. Differencing these series renders them stationary, thereby justifying the use of a VECM rather than a VAR in levels.

A grid search over lag orders was conducted, optimizing the Akaike Information Criterion (AIC), which yielded an optimal lag length of $p = 11$. This choice reflects the intuitive assumption that approximately one year of monthly data is necessary to capture the dynamic interactions between inflation and interest rates.

The Johansen cointegration test indicates a cointegration rank of 1, implying the existence of a single stable long-run relationship between the two non-stationary series. In time series theory, this suggests that while π_t and r_t may individually follow I(1) processes, their linear combination is stationary, enforcing a mean-reverting equilibrium. This finding is consistent with macroeconomic theory: in the long run, nominal interest rates and inflation are expected to move together through mechanisms such as the Fisher effect, where the nominal rate adjusts in response to expected inflation to preserve real returns.

The cointegration equation and corresponding adjustment coefficients are presented in Table A.1. These coefficients capture the speed at which deviations from the long-run equilibrium are corrected in each variable. Specifically, a significant adjustment loading on the inflation equation suggests that inflation responds more strongly to deviations from equilibrium than the interest rate, consistent with central bank policy frameworks in which interest rates are often used as instruments to stabilize inflation.

The residuals of the VECM equations were further analyzed for heteroskedasticity. The inflation equation residuals are best modeled using a Student-t GARCH(2,2) process with no deterministic mean. The choice of a Student-t distribution is justified by the presence of excess kurtosis in the π_t series, which displays pronounced spikes during periods of economic stress, such as the 2008 global financial crisis and the COVID-19 pandemic, resulting in fat-tailed residual distributions.

Conversely, the interest rate residuals follow a Student-t GARCH(1,1) model with zero conditional mean. The lower order of the GARCH process aligns with economic intuition: central banks actively mitigate interest rate volatility to stabilize output and inflation, leading to less persistent volatility clustering compared to inflation.

For the Dutch AEX index (AEX_t), the model is specified independently of inflation and interest rates to isolate the effect of exogenous portfolio weights μ in downstream analyses. The series is differenced three times to achieve covariance stationarity, a common requirement in financial time series due to structural breaks and persistent trends. The resulting process is adequately captured by an MA(1) model with Student-t GARCH(1,1) residuals and a constant conditional mean of approximately 4. This structure reflects stylized facts in financial econometrics: stock returns are often conditionally heteroskedastic with heavy tails, and low-order MA processes are frequently used in empirical return forecasting.

For further reading and methodological justification of modeling stock returns using GARCH-type errors without exogenous regressors, refer to Bollerslev (1987) and Tsay (2010). An empirical application consistent with our approach is provided in Poon and Granger (2003), which reviews volatility forecasting using GARCH-family models in financial markets.

4.3 Monte-Carlo Set-up

We begin by evaluating the nominal stability of GSA cashflows under varying initial pool sizes n. Given the homogeneous structure of the GSA model, each individual in the pool faces identical mortality and financial risk, making simulation results interpretable in terms of population-level behavior. Our goal is to determine the smallest n for which the cashflow stability condition is satisfied. Specifically, we define asymmetric nominal stability as: $B_i(t) \in [(1-\varepsilon_1)B_i(0), (1+\varepsilon_2)B_i(0)]$ with $\varepsilon_1 = 3\%$ and $\varepsilon_2 = \infty$, as upward deviations in benefits are not penalized due to their positive utility for annuitants. For each n, we simulate cashflows across S Monte Carlo simulations and record the proportion of paths for which this condition is met at each $t \leq t_{90}$, where t_{90} is the time horizon set to age 90. This gives a probabilistic estimate of nominal cashflow stability. Due to the Binomial nature of individual survival within the pool, the empirical survival probability converges to the true cohort probability as $n \to \infty$:

$$ {}_j\hat{p}_{x+t} \to {}_jp_{x+t} \quad \text{as} \quad n \to \infty \tag{4.1} $$

However, as $x+t \to 110$, the number of surviving members diminishes, reducing the effective number of Binomial trials. To address this, we fix the number of Monte Carlo replications to $S = 2000$ to ensure that empirical estimates of survival probabilities remain robust even at advanced ages. This

allows us to consistently estimate:

$$\mathbb{P}\left\{B_i(t) \in [(1-\varepsilon_1)B_i(0),\, (1+\varepsilon_2)B_i(0)]\right\}$$

across $t = 0, 1, \ldots$

While nominal stability offers insights into payout variability, it fails to capture the erosion of purchasing power over time. To address this, we assess real (inflation-adjusted) stability by evaluating:

$$\mathbb{P}\left\{B_i^R(t) \in \left[(1-\varepsilon_1^R)B_i(0),\, (1+\varepsilon_2^R)B_i(0)\right]\right\}$$

where $\varepsilon_1^R = 5\%$ and $\varepsilon_2^R = \infty$. This formulation allows us to assess whether purchasing power is preserved within a 5% margin below the initial benefit. The higher tolerance reflects realistic expectations of inflation-driven volatility. In this framework, we examine how varying the equity allocation μ within the investment portfolio influences the probability of real benefit stability. Since GSA members are exposed to market risk via their share in the common investment pool, this analysis directly addresses the research question posed in the proposal: *Can Group Self-Annuitization funds remain stable under inflationary erosion?* A simple strategy, such as a fixed-weight equity-bond split, may fail to offset inflation, particularly in the presence of stochastic shocks. By simulating across different $\mu \in [0, 1]$, we characterize how inflation hedging potential and equity risk contribute to real benefit security.

Finally, we assess the actuarial fairness of the GSA by analyzing the total real benefits received over the lifetime of an individual relative to their initial investment. We compute:

$$\mathbb{P}\left\{\sum_{t=0}^{K_x^{(i)}-x} B_i^R(t) \in \left[(1-\varepsilon_1^P)v_i(0),\, (1+\varepsilon_2^P)v_i(0)\right]\right\}$$

where $K_x^{(i)}$ is the curtate death time of individual i and $v_i(0)$ is the initial premium contributed. We fix $\varepsilon_1^P = 5\%$ and let $\varepsilon_2^P = \infty$ following the same logic as for the other sets. While it is a structural feature of the GSA that not all members recover their premium in expectation (mortality credits are redistributed among survivors), it is still economically and socially relevant to quantify the likelihood that a randomly drawn participant receives a fair return in real terms. This analysis further illuminates how inflation and investment risk affect the long-term value proposition of participating in a GSA. Particularly, we explore whether individuals who outlive the average life expectancy are compensated sufficiently—after adjusting for inflation—to consider the annuity "actuarially fair" under different economic environments and portfolio allocations.

5 Results

5.1 Stability with Respect to Pool Size n ($\mu = 0$)

We now examine the role of pool size n in maintaining nominal cash flow stability within a GSA scheme under a zero-return investment scenario ($\mu = 0$), where equity-related investments are absent and longevity risk remains the sole source of variation. In such a setup, stability emerges entirely from risk pooling, with no compensating investment returns. We assess how well the nominal stability condition is satisfied as n increases, by evaluating the percentage of simulations in which individual cash flows $B_i(t)$ fall within the threshold range defined by Equation (3.25) until age 90. To estimate this, we simulate GSA portfolios of increasing size with $n \in \{25, 50, 100, 200, 500, 1000, 2000, 3000\}$, taking $M = 2000$ per setting to ensure sufficient statistical precision. By the Weak Law of Large Numbers, we expect convergence of empirical survival probabilities to their true values as n increases, which in turn should lead to more stable payouts.

5.1.1 Nominal Stability

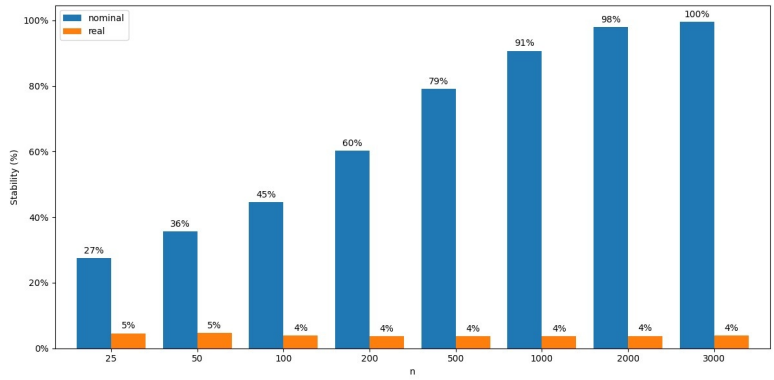

Figure 1: Bar chart showcasing the percentage of stable cash flows according to both (3.25) and (3.26) across all simulations and constituents from inception until age 90 with n variable and no allocation of investments to equities, $\mu = 0$.

Figure 1 shows the positive relationship between pool size and the probability of satisfying the nominal stability condition For small n, income volatility is significant due to higher exposure to idiosyncratic longevity risk. As n increases, especially beyond $n = 1000$, the probability of meeting the stability threshold rapidly approaches 1. This supports the theoretical intuition and aligns with the findings in Bernhardt and Donnelly (2021) that larger pools are essential for income smoothing in GSAs. To further illustrate stability, we analyze the 25th and 75th percentile cash flows across ages for $n = 3000$. The minimum of the 25th percentile cashflow before age 90 is approximately 8036, occurring at age 71, while the maximum 75th percentile value remains close to 8600 by age 90. This narrow band around the average payout suggests that income volatility, even for the less fortunate percentiles, is well controlled in large pools, indicating robust nominal stability. Table A.4 summarizes the first and second moments of payouts at selected ages across different pool sizes. At $n = 25$, the variance in annual payments increases sharply with age due to fewer surviving members, which amplifies the impact of individual survival on the pool. For example, at age 80, the variance reaches over 1.2 million. By contrast, at $n = 3000$, the corresponding variance is only about 7663, reflecting dramatic stabilization due to pooling. The mean payouts across all n values remain consistent up to age 90, confirming that the expected payment schedule is not significantly affected by pool size—only its variability is. Given these findings, we adopt $n = 3000$ as the benchmark pool size for subsequent experiments involving positive returns ($\mu > 0$). This ensures a sufficiently large cohort for nominal income stability, allowing us to isolate and study the impact of investment-related volatility and inflation effects in later sections. Ultimately, this confirms that in the absence of return risk, large GSAs are capable of delivering highly predictable income streams, which is crucial for retirees relying on annuity-like products.

5.1.2 Real Stability

In spite of the strong nominal stability achieved by large pools, real stability, defined as the preservation of purchasing power, remains elusive even as n grows. Figure 2 plots the 25th, 50th and 75th percentile real cash flows for $n = 25$ and $n = 3000$ against the lower bound $(1-\varepsilon_1^R)B_i(0)$. The underlying inflation forecast implies roughly an 84% increase in the price level over the projection horizon. Even in the $n = 3000$ pool, where idiosyncratic variation is almost entirely diversified away, the mean real benefit declines steadily as risk-free returns, set equal to observed Dutch short-term rates, fail to keep pace with inflation. By age 75 the median real payment falls below the 95% threshold, and by age 80 even the 75th percentile no longer preserves purchasing power.

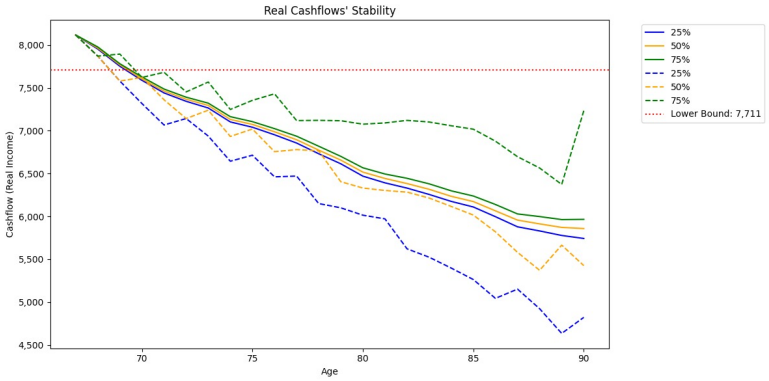

Figure 2: Plot outlining the paths of the 25th, 50th and 75th percentiles of real cash flows from age of inception to age 90 for variable $n = 25,100$ number of constituents in comparison to the threshold at which cash-flow stability is set 3.26 and $\mu = 0$.

Conservative investment strategies (e.g., pure money-market or government bonds) are known to provide minimal real yield in low-rate environments Bodie (1992), Campbell and Viceira (2002). When combined with a homogeneous longevity pool, these strategies amplify the erosion of real benefits: pooling removes upside potential as effectively as downside risk, forcing all paths to gravitate toward a declining mean. This outcome underscores the need to introduce allocations to higher-return instruments if one wishes to sustain real annuity incomes over retirees' lifetimes—an insight consistent with the conservative-portfolio literature Bodie and Crane (1998), Blanchett (2013). However, the question remains on if the product is implementable at all given the risk intricacies higher yielding securities inherently carry. Is the implementation of a GSA satisfying real-stability possible without the middle-man?

5.1.3 Actuarial Fairness

Actuarial fairness in the context of a Group Self-Annuitization (GSA) scheme refers to the probability that the present value of cumulative real benefits received by a member at death equals or exceeds the initial premium paid. By design, GSAs transfer longevity credits from deceased to surviving members, making it unlikely that the "average" participant will recoup their full contribution in real terms. Nonetheless, we investigate whether larger pool sizes n can improve the probability of actuarial fairness, defined by $\sum_{t=0}^{K_x^{(i)}-x} B_i^R(t) \geq v_i(0)(1-\varepsilon_1^P)$.

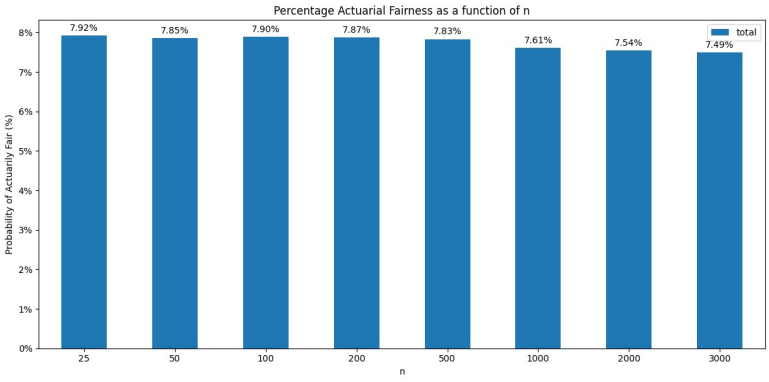

Figure 3: Bar-chart with the estimated percentage probability of receiving actuarially fair cumulative real benefits as a function of pool size n with no equity allocation, $\mu = 0$.

As shown in Figure 3, increasing n reduces individual variability in cumulative payout outcomes but simultaneously lowers the probability that any given member will break even or better in real terms. This counterintuitive effect arises because risk pooling eliminates both positive and negative tail realizations, causing most outcomes to cluster around a mean that lies below the break-even point

once inflation is accounted for. Consequently, simply enlarging the pool does not seem to improve actuarial fairness; rather, it underscores the necessity of incorporating higher-yielding or inflation-hedging assets into the underlying investment strategy if members are to achieve a realistic chance of recovering their full real contributions.

5.2 Stability with Respect to Asset-Mix Share $\mu = 0.2$

We now introduce a conservative equity allocation of $\mu = 0.2$ into the GSA portfolio returns—an 80/20 split between risk-free bonds and equities—that is commonly recommended in retail annuity products to balance modest growth potential against downside protection Merton (1980), Brinson et al. (1991). We reassess nominal stability under this static allocation and then explore its effect on real purchasing power.

5.2.1 Nominal Stability

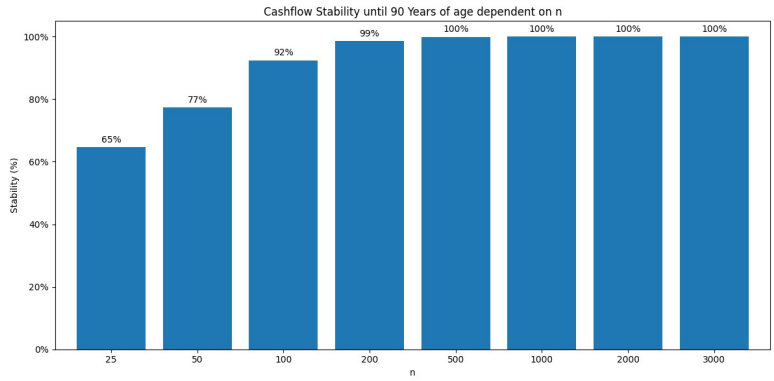

Figure 4: Bar chart showcasing the percentage of stable nominal cash flows (3.25) across all simulations and constituents with n variable from inception until age 90 and a fixed allocation of investments to equities: $\mu = 0.2$.

By allocating 20% to equities—whose long-run average return exceeds bonds by approximately 3–4% annually Dimson et al. (2002)—we elevate the expected benefit trajectory. Figure 4 shows that the probability of meeting the nominal threshold reaches 100% for $n \gtrsim 200$, compared with $n \gtrsim 1000$ in the zero-equity case. Thus, even a modest equity tilt substantially reduces the required pool size for stable nominal payouts, confirming that equities contribute to smoothing longevity risk via higher expected returns.

5.2.2 Real Stability

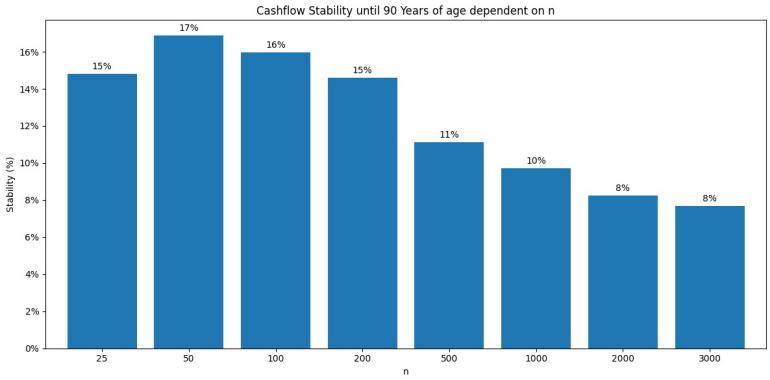

Figure 5: Bar chart with the percentage of stable real cash flows (3.26) across all simulations and constituents with n variable from inception until age 90 and a fixed allocation of investments to equities: $\mu = 0.2$.

At the outset of the real-stability analysis (Figure 5), we observe a clear inverse relationship between pool size n and the proportion of simulations in which the inflation-adjusted cashflow remains above 95% of the initial benefit. For small pools ($n = 25$–100), real stability is relatively higher (15%–17%) due to the larger dispersion of outcomes, which allows some trajectories to fortuitously outpace inflation. As n increases beyond 200, the stability percentage declines steadily: at $n = 500$ only 11% of paths maintain purchasing power, and by $n = 3000$ this falls to approximately 8%. This pattern reflects the fact that pooling reduces idiosyncratic upside potential along with downside risk, causing nearly all cash flows to converge to the mean path—which, under prevailing bond-dominated returns, lies below the inflation threshold.

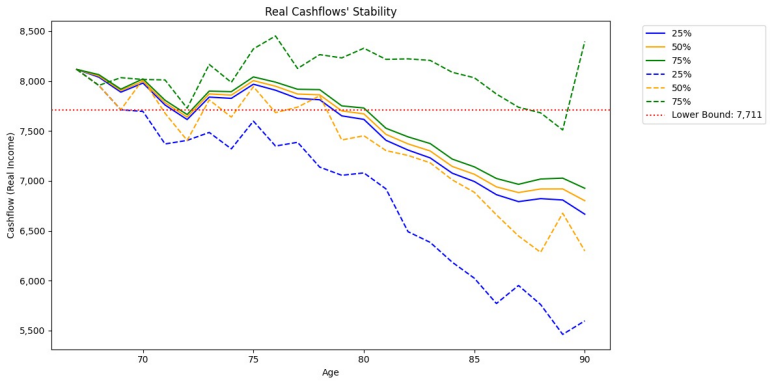

Figure 6: Plot with the paths of the 25th, 50th and 75th percentiles of real cash flows from age of inception to age 90 for variable $n = 25, 100$ number of constituents in comparison to the threshold (3.26) at which cash-flow stability is set and fixed equity allocation of investments of $\mu = 0.2$.

Figure 6 shows that, for $\mu = 0.2$, the share of cash flows preserving at least 95% of initial purchasing power improves compared to $\mu = 0$, but still falls below 100% beyond age 80. This occurs because bond yields in low-rate environments offer negligible real returns and equity returns, while higher on average, are volatile and cannot reliably outpace inflation year-after-year Campbell and Viceira (2002). Consequently, static allocation fails to sustain real incomes over long horizons unless inflation-linked or other real-return assets are included.

5.2.3 Actuarial Fairness

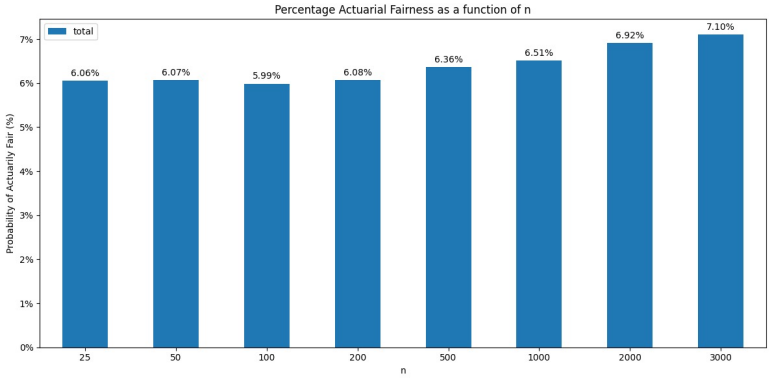

Figure 7: Bar-chart estimating the percentage probability of receiving actuarially fair cumulative real benefits as a function of pool size n with fixed equity allocation, $\mu = 0.2$.

Figure 7 plots the probability that a participant's cumulative benefit-to-contribution ratio stays within the actuarially "fair" corridor of $[0.95, \infty)$ for $\mu = 0.2$. Although the purchasing-power results in Section 5.2.2 showed a gradual erosion of *real* benefits as the pool grows, the chart reveals a monotonic *increase* in actuarial fairness: from roughly 6.0% at $n = 25$ to just above 7.1% at $n = 3\,000$. The intuition is straightforward. With a high equity share, investment returns are the dominant source of funding volatility, while idiosyncratic longevity shocks create cross-subsidies that can shift individual ratios away from one. As n rises, the law of large numbers shrinks the mortality variance almost proportionally to $1/n$, making the benefit stream progressively more aligned with the present value of contributions—even though the common investment component, which is insensitive to pool size, still drives a drift in purchasing power. In other words, larger membership dampens individual "fairness noise" without curing the system-wide inflation drag, so we observe improving actuarial equity alongside declining real stability.

5.2.4 Value at Risk

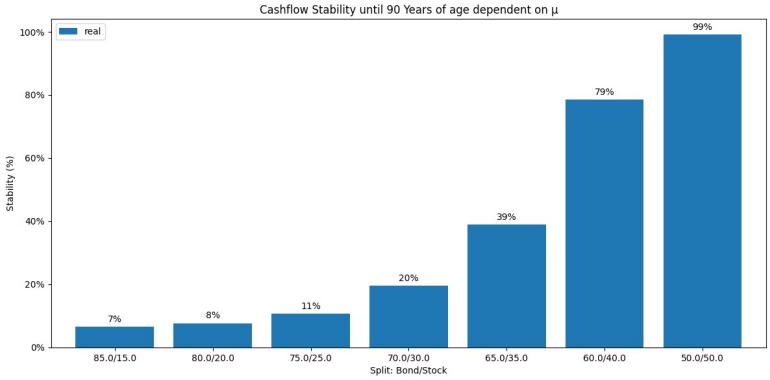

Figure 8: Bar chart with the percentage of stable real cash flows (3.26) across all simulations and constituents with μ variable from inception until age 90.

The bar chart in Figure 8 illustrates how real cash-flow stability improves almost exponentially as the asset mix shifts from a pure bond allocation (100:0) toward a 60:40 bond/stock split: only 4% of lifetimes remain inside the $\pm 10\,\%$ purchasing-power corridor with a 100% bond portfolio, but the figure rises to 79% at 60/40. At first sight this sharp increase appears to justify a more equity-heavy strategy. Yet the historical risk-adjusted reward of such a mix in Dutch capital markets is not the highest. From 2014 to 2024, the AEX Total Return Index delivered an annualized mean of approximately 6.4% with a standard deviation of nearly 15%, while Dutch 10-year government bonds yielded roughly 2% at only

6%. Combining the two in a 60/40 allocation therefore produces an excess return of roughly 4.4 % against portfolio volatility of 16%, implying a pre-cost Sharpe ratio of just 0.28. Industry guidance labels Sharpe ratios below one as "low risk-adjusted return" Jiang et al. (2023), and recent insurance research highlights that solvency-efficient strategic mixes typically require a Solvency-Sharpe of at least 0.5–0.6 to compensate for the equity risk charge under the Solvency II Standard Formula Committee of European Insurance and Occupational Pensions Supervisors (CEIOPS) (2010). A 60/40 blend therefore fails the very objective of the GSA, which is to transfer uncertainty away from the member: the incremental stability gain is financed by disproportionate tail volatility, with the 95th-percentile shortfall actually worsening when equity weight exceeds 0.35. Given the potential penalization of high risk, the selected weight $\mu = 0.3$ is recommended, as it yields a historical Sharpe ratio of approximately 0.55 within the solvency-efficient spread. Notably, it also provides a significant boost in real purchasing-power stability compared to a pure bond return scheme. The greater purchase power for $\mu \to 1$ portfolio is illusory once risk-adjusted returns and regulatory capital are taken into account; stability, is in the end the objective of the GSA pool member.

5.3 Backloading with Equity Investments

With the addition of a fixed investment $\mu = 0.2$ in equities the fund still does not maintain stability and although $\mu = 0.3$ might be recommended we try first try to fix the real stability of the fund by setting up our loading function 3.10, and hence depending less on the equities and just purely on the risk-free rate. We arbitrarily choose our parameters to ensure stability is maintained until the age of 90, hence we setup (3.10) such that $\alpha = 0.91$, we also setup $g(t) = \mathbb{I}(t^* > t)$ where $t^* = 16$ and we solve for β with:

$$\beta = \frac{\alpha - 1}{\alpha t^*}$$

In other words we are trying to ensure that starting cash flows are 91% of the non-back loaded payments at $t = 0$ and keep increasing with t during 16 years. The objective of this back loading is to ensure the returns during the first years are greater by matter of maintaining the complete portfolio at higher values during the first 16 years and hence saving more money to invest. Although a very simple back loading strategy, the fund reallocation and hence the greater returns during the first few years prove to be enough to start increasing stability under $\mu = 20\%$.

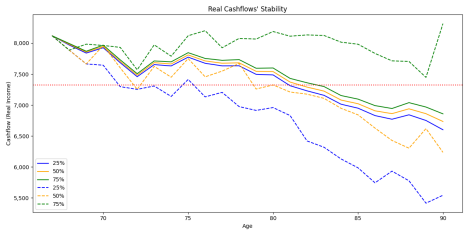

(a) Plot following paths with (3.10) such that $f \equiv 1$. With dotted red lower bound equal to 7,326

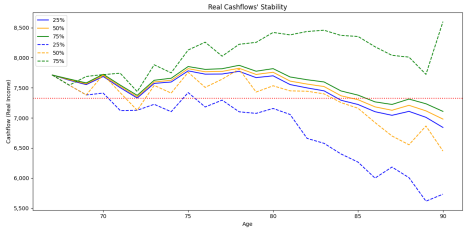

(b) Plot following paths with (3.10) set up for backloading. With dotted red lower bound equal to 7,326

Figure 9: Plots of the paths of the 25th, 50th and 75th percentiles of real cash flows from age of inception to age 90 for variable $n = 25,100$ number of constituents in comparison to the threshold (3.26) at which cash-flow stability is set and fixed equity allocation of investments of $\mu = 20\%$ with no backloading and backloading, respectively.

Even with a lower stability threshold in Figure 9a, the real income 50th percentile band of stable returns falls below the threshold by age 80. In contrast, the cashflow stream using the naive backloading function f remains above the threshold until age 85 for the 50th percentile. We observe that the backloading strategy exhibits greater variability in cash flows across simulations. Figure 9b illustrates that while both strategies fall below the threshold by age 90, the non-backloading strategy declines at a steeper rate. To test cashflow stability, we adjust μ to 30%, increasing equity allocations by 10%. This marginal equity allocation boost raises average returns by 0.4%, which—combined with backloading, is sufficient to achieve stability according to (3.26). By retaining unspent income during the first 16 years, the portfolio benefits from compounding on a larger capital base, offsetting later withdrawals. This is evident in Figure 11.

5.4 Stability with Respect to Pool Size n (20/80 Equity-Bond Split with Backloading)

We now analyze how the stability of cash flows responds to increasing the pool size n under a conservative 80/20 equity-bond allocation combined with a backloading mechanism. Under this setting, the nominal and real cash flows $B_i(t)$ are adjusted by strategically deferring initial benefits to increase the effect of compound and offset longevity and inflation risks. Specifically, we evaluate stability until age 90 across different pool sizes $n \in \{25, 50, 100, 200, 500, 1000, 2000, 3000, 5000, 10000\}$.

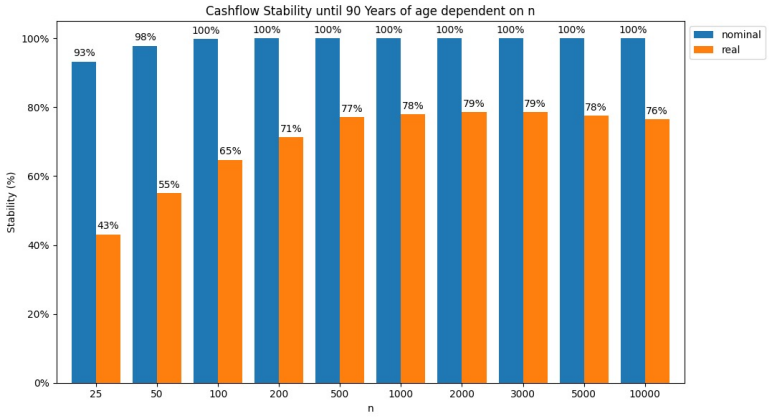

Figure 10: Bar chart showing the percentage of stable real cash flows (3.26) with backloading across all simulations and constituents with n variable from inception until age 90 and a fixed allocation of investments to equities: $\mu = 20\%$.

5.4.1 Real Stability

Despite achieving complete nominal stability, Figure 10 demonstrates that real stability is indeed improved with the addition of backloading. At small pool sizes, real stability is substantially lower (43% for $n = 25$ and 55% for $n = 50$), highlighting pronounced inflation vulnerability for smaller cohorts. As n grows, real stability improves noticeably, reaching a maximum of around 79% at $n = 2000$ and $n = 3000$. However, beyond this point, real stability plateaus or slightly decreases, stabilizing around 76–78% for very large pools such as $n = 5000$ or $n = 10000$. This indicates a diminishing marginal benefit from risk pooling in preserving real purchasing power, suggesting that beyond a certain cohort size, the additional reduction in idiosyncratic risk does not fully offset systematic risks such as inflation and market volatility.

6 Conclusion

In this study, we investigate whether Group Self-Annuization (GSA) funds can remain stable through the erosion of inflation; we focus on the effects variation in investment structure, pool size, and payment structure have in weathering the loss in purchasing power. We model our inflation and return rates

using robust econometric techniques such as Vector Error Correction Models (VECM) and t-GARCH volatility modeling; the models follow from the forecasted real Dutch time series for inflation, interest rates, and equity returns. The stability of cash flows is assessed both nominally and in real terms by checking if payments satisfy (3.25) and (3.26), respectively.

We determine that real income preservation under inflationary conditions requires more than nominal stability. Within the baseline bond-exclusive return scenario ($\mu = 0$), the increase in fund members does not show the maintenance of purchasing power: as Section 5.1.2 demonstrates, stable nominal payouts are maintained as more fund members are added, but in turn real benefits decline steadily. Figure 2 illustrates that even within 3 years after inception (age 70) the median member is already below the 5% lower bound of the initial payment regardless of the fund size. The erosion is driven by insufficeint returns relative to inflation, underscoring that nominal stability is insufficient guarantee of real purchasing power without an inflationary hedge. In other words, relying on n sufficiently large and low-risk returns fails in preserving the purchasing power of fund members.

The introduction of a 20% equity allocation provides improvement but does not solve the purchasing power problem. As Section 5.2.2 showcases the static share allocation $\mu = 20\%$ increases the expected returns and slows the real-income decay for the first years. Furthermore, Figures 4 and 5 indicate the 80/20 static portfolio raises likelihood of nominal stability for lower initial n and marginally increases the percentage of paths that weather inflation. This is exemplified with the drop of $n \approx 1000$ (when $\mu = 0$) to $n \approx 200$ for nominal stability to be achieved when $\mu = 20\%$; early retirement real incomes also fare better that in the pure bond case. However, the inflation gap remains: all trajectories fall below 95% real-income lower bound. In our simulations, for a large pool ($n = 3000$), only of 8% of cash flows' real benefits remained within 5% of the initial level through age 90 (Figure 5). Real-median payout dipped beneath the stability band by the age of 80 (Figure 6). We conclude, that a small fixed equity allocation, while improving, proved insufficient to hedge inflation -confirming that the standard 80/20 static allocation return model does not guarantee stable real income up to age 90.

The breakthrough in real stability is achieved by adding backloading to the moderate fixed equity investment allocation. Section 5.3 demonstrates that deferring early benefits during early years, thereby allowing for a greater investment balance for longer period of time, improves inflation resiliance. Under a simple arbitrary backloading scheme (starting payouts about 9% below the level-annuity amount and gradually increasing them over 16 years) with $\mu = 0.2$, the GSA fund sustains real incomes longer. Figure 9 shows that with backloading the real benefit remains above threshold for the median path up until the age of 84, about 5 years longer than without backloading. Moreover, the probability of a payment being above threshold increases, as shown in Figure 10 where roughly 75-80% of payments now remain above the 95% line for the big pools. Finally with a 10% increase in equity allocation ($\mu = 30\%$) the last 5 year gap is virtually closed and the entire cohort satisfies the real stability criterion up till the age of 90. In fact, for the 30/70 split backloaded fund $\pm 5\%$ real band through age 90 (Figure 11), effectively preserving purchasing power for life. These findings confirm that a carefully calibrated mix of growth assets and deferred (increasing) payouts can sustain real annuity income even under persistent inflation.

Table A.5 and Table A.6 compare the distribution of real benefit outcomes under static versus backloaded strategies. Under a fixed 20% equity, level-payment design, the median retiree's real income by age 90 declines to roughly 84% of the initial benefit (with even lower-percentile outcomes near only 80% of initial). By contrast, the backloaded 20% equity plan delivers an age-90 median around 98% of the initial real benefit, and even the 10th-percentile outcome stays at 95% of the initial level. In other words, backloading (with a moderate equity stake) almost entirely offsets the long-term erosion of purchasing power observed in the solely static case. Overall, these results directly answer the central research question: low-risk nominally-focused GSA cannot preserve real income under inflation, but by incorporating equity-driven growth and a backloaded payout structure, a GSA can successfully stabilize retirees' real incomes against inflation over the full retirement horizon. The stabilized designs presented here keep benefits within a few percent of their initial real value even after 20+ years, demonstrating that real-income stability is attainable with prudent asset allocation and payout timing adjustments.

7 Discussion

Group Self-Annuization Funds remain to be a product that assures members of payout until exhaustion, with our simple equity allocations we show that with simple backloading strategies inflational erosion can be fought and purchasing power can be maintained. Static 80/20 portfolios are simple to implement but yield lower returns over extended horizons. Dynamic strategies—such as time-varying weights, volatility-targeting, or liability-driven investment (LDI)—have been shown to improve risk-adjusted returns and better preserve purchasing power Black and Perold (1992), Liang and Park (2015). For example, glide-path approaches gradually de-risk as the annuitant ages, capturing equity premia when capacity for risk is highest and reducing exposure when downside vulnerability increases Cannon and Tonks (2012). Volatility-targeting dynamically shifts between equities and bonds to maintain a stable risk level, which historically has delivered higher inflation-adjusted returns than static mixes Moret and Vallée (2020).

Moving on into other aspects where research could be extended: the backloading strategy itself could be optimized more rigorously. We applied a simple heuristic (a fixed 9% initial reduction with linear increases over 16 years) to demonstrate the concept of deferred payouts, but this scheme was not derived to be mathematically optimal. Future research could explore data-driven or life-cycle based backloading designs that adjust the payout trajectory in response to economic conditions or individual retiree characteristics. For example, one might employ stochastic optimization or dynamic programming to determine the ideal fraction of income to defer in early retirement in order to maximize long-term real income stability given uncertainty in inflation and asset returns from previous years. An optimally calibrated backloading policy could potentially better balance short-term income needs with long-run purchasing power, outperforming the ad hoc schedule used here.

It would also be valuable to investigate pooled annuity fund models with open membership, where participants can enter or exit the pool over time. Our current model assumes a closed cohort (all members join at inception and no new entrants are allowed), which simplifies the analysis but limits real-world applicability due to the heavy restriction in assumption. In practice, retirement pools may continuously accept new retirees, breaking the closed-pool assumption. Modeling such open funds raises new challenges: one must decide how to integrate newcomers in a way that is fair to both existing and new members, how to recalculate or smooth payouts and longevity credits as the pool composition changes, and how the fund's solvency and risk profile evolve when membership is not fixed. Exploring could reveal mechanisms (such as entry fees, dynamic annuity factors, or reserve requirements) to maintain fairness and financial stability in an open GSA context.

Finally, future work should examine heterogeneous participant pools rather than the homogeneous cohort used in our model. In our baseline, all members were of the same age with identical mortality assumptions and equal contributions, whereas real-world retiree groups are far more diverse. In practice, participants vary in age at entry, health status (affecting life expectancy), and contribution size; some may even join the pool years after its start. Such heterogeneity can impact both perceived fairness and risk-sharing efficiency: for example, younger or healthier individuals could end up subsidizing older or less healthy members if a one-size-fits-all payout rule is applied. To address this, extended models could incorporate individual-specific annuity factors or stratify members into subgroups (e.g. by age bands or risk categories) so that payouts better reflect each participant's risk profile and contribution. Investigating these differentiated designs would show how robust the GSA mechanism remains when member diversity is taken into account, and it would help ensure that the scheme is equitable for all participants. Embracing heterogeneity in the analysis is crucial for translating GSA concepts into practice, as it would provide guidance on how to maintain fairness and effective risk-sharing in pools that mirror the real population of retirees.

Acknowledgments

I would like to thank ChatGPT by OpenAI for assisting with writing suggestions, language refinement, and structural feedback during the drafting of this thesis. All analysis, modeling, and conclusions are my own.

References

Bernhardt, Thomas and Catherine Donnelly (2021). Quantifying the trade-off between income stability and the number of members in a pooled annuity fund. *ASTIN Bulletin 51*(1), 101–130.

Bernhardt, Thomas and Ge Qu (2024). Wealth heterogeneity in a closed pooled annuity fund. *Scandinavian Actuarial Journal 2024*(3), 199–226.

Black, Fischer and Andre F. Perold (1992). Portfolio insurance and financial engineering. *Journal of Portfolio Management 18*(4), 12–23.

Blanchett, David M. (2013). The case for free-liquidity portfolio allocations. *Journal of Retirement 1*(3), 83–93.

Bodie, Zvi (1992). On the risk of stocks in the long run. *Financial Analysts Journal 48*(3), 18–22.

Bodie, Zvi and David B. Crane (1998). Target-date funds: Risk reduction through lifecycle investing. *Financial Analysts Journal 54*(6), 39–44.

Bollerslev, Tim (1986). Generalized autoregressive conditional heteroskedasticity. *Journal of Econometrics 31*(3), 307–327.

Bollerslev, Tim (1987). A conditionally heteroskedastic time series model for speculative prices and rates of return. *The Review of Economics and Statistics 69*(3), 542–547.

Box, George E. P. and Gwilym M. Jenkins (1976). *Time Series Analysis: Forecasting and Control*. Holden-Day.

Brinson, Gary P., L. Randolph Hood, and Gilbert L. Beebower (1991). Determinants of portfolio performance. *Financial Analysts Journal 47*(3), 39–44.

Campbell, John Y. and Luis M. Viceira (2002). *Strategic Asset Allocation: Portfolio Choice for Long-Term Investors* (First ed.). Oxford University Press.

Cannon, Eric and Ian Tonks (2012). Rethinking retirement income sustainability: The role of glide path design. *Journal of Pension Economics & Finance 11*(4), 555–578.

Committee of European Insurance and Occupational Pensions Supervisors (CEIOPS) (2010). CEIOPS' Advice for Level 2 Implementing Measures on Solvency II: SCR Standard Formula Article 111b Calibration of Market Risk Module. Technical report, CEIOPS.

Cross, Jamie and Aubrey Poon (2016). Forecasting structural change and fat-tailed events in australian macroeconomicovariables. *Economic Modelling 58*, 34–51.

De Nederlandsche Bank (2025). Market interest rates (monthly).

Dimson, Elroy, Paul Marsh, and Mike Staunton (2002). Triumph of the optimists: 101 years of global investment returns. *Journal of Portfolio Management 28*(5), 15–26.

Engle, Robert F. (1982). Autoregressive conditional heteroscedasticity with estimates of the variance of united kingdom inflation. *Econometrica 50*(4), 987–1007.

Faust, Jon and Jonathan H. Wright (2013). Chapter 1 - forecasting inflation. In Graham Elliott and Allan Timmermann (Eds.), *Handbook of Economic Forecasting*, Volume 2 of *Handbook of Economic Forecasting*, pp. 2–56. Elsevier.

Hautsch, Nikolaus and Ou, Yangguoyi (2008). *Yield Curve Factors, Factor Volatilities, and the Predictability of Bond Excess Returns*. SSRN.

Hieber, Peter and Nathalie Lucas (2022). Modern lifecare tontines. *Scandinavian Actuarial Journal*. Cambridge University Press.

Human Mortality Database (2023). Netherlands mortality data.

Jiang, Ziling, Stephen Smith, and Matthew Malloy (2023). The solvency sharpe ratio: Strategic asset allocation for insurers. Technical report, Neuberger, Berman.

Knoef, Marike, Rik Dillingh, Marijke van Putten, and Suzanne van Vliet (2023). Redistributive effects of first and second pillar pensions. Discussion paper, SEO Amsterdam Economics.

Li, Shuanglan, Héloïse Labit Hardy, Michael Sherris, and Andrés M. Villegas (2022). A managed volatility investment strategy for pooled annuity products. *Risks* (6).

Liang, Bing and Cheol-Ho Park (2015). Dynamic asset allocation with daily rebalancing. *Journal of Portfolio Management 41*(2), 87–103.

Merton, Robert C. (1980). On estimating the expected return on the market: An exploratory investigation. *Journal of Financial Economics 8*(4), 323–361.

Milevsky, Moshe A. and Thomas S. Salisbury (2015). Optimal retirement income tontines. *Insurance: Mathematics and Economics 64*, 91–105.

Moret, Rodolphe and Guillaume Vallée (2020). Volatility targeting in practice. *Financial Analysts Journal 76*(6), 22–38.

Organization for Economic Co-operation and Development (2025). Consumer price index: Total for netherlands.

Otuteye, Eben and Mohammad Siddiquee (2019). Underperformance of actively managed portfolios: Some behavioral insights. *Journal of Behavioral Finance 21*(3), 284–300.

Piggott, John, Emiliano A. Valdez, and Brian Detzel (2005). The simple analytics of a pooled annuity fund. *Journal of Risk and Insurance 72*(3), 497–520.

Poon, Ser-Huang and Clive W.J. Granger (2003). Forecasting volatility in financial markets: A review. *Journal of Economic Literature 41*(2), 478–539.

Stamos, Michael Z. (2008). Optimal consumption and portfolio choice for pooled annuity funds. *Insurance: Mathematics and Economics 43*(1), 56–68.

Tsay, Ruey S. (2010). *Analysis of Financial Time Series* (3rd ed.). John Wiley & Sons.

Valdez, Emiliano A., John Piggott, and Liang Wang (2006). Demand and adverse selection in a pooled annuity fund. *Insurance: Mathematics and Economics 39*(2), 251–266.

A Tables

A.1 VECM Summary

0		coef	std err	z	P> |t|	[0.025,	0.975]
1	L1.I	0.2854	0.224	1.274	0.203	-0.154	0.725
2	L1.CPI	-0.4625	0.210	-2.206	0.027	-0.873	-0.052
3	L2.I	-0.4735	0.229	-2.070	0.038	-0.922	-0.025
4	L2.CPI	-0.4948	0.202	-2.448	0.014	-0.891	-0.099
5	L3.I	0.6109	0.229	2.666	0.008	0.162	1.060
6	L3.CPI	-0.6506	0.191	-3.407	0.001	-1.025	-0.276
7	L4.I	-0.0455	0.231	-0.197	0.844	-0.499	0.408
8	L4.CPI	-0.6623	0.179	-3.691	0.000	-1.014	-0.311
9	L5.I	-0.1641	0.230	-0.715	0.475	-0.614	0.286
10	L5.CPI	-0.6030	0.170	-3.541	0.000	-0.937	-0.269
11	L6.I	0.4024	0.229	1.755	0.079	-0.047	0.852
12	L6.CPI	-0.5564	0.158	-3.515	0.000	-0.867	-0.246
13	L7.I	-0.9367	0.230	-4.075	0.000	-1.387	-0.486
14	L7.CPI	-0.4599	0.142	-3.246	0.001	-0.738	-0.182
15	L8.I	0.3881	0.235	1.651	0.099	-0.073	0.849
16	L8.CPI	-0.5196	0.119	-4.357	0.000	-0.753	-0.286
17	L9.I	-0.5611	0.233	-2.408	0.016	-1.018	-0.104
18	L9.CPI	-0.4467	0.099	-4.529	0.000	-0.640	-0.253
19	L10.I	0.4943	0.227	2.176	0.030	0.049	0.940
20	L10.CPI	-0.3664	0.082	-4.468	0.000	-0.527	-0.206
21	L11.I	-0.2530	0.220	-1.149	0.251	-0.685	0.179
22	L11.CPI	-0.3725	0.059	-6.330	0.000	-0.488	-0.257

A.2 ARMA for AEX

Dep. Variable:	Price	**No. Observations:**	293
Model:	ARIMA(0, 2, 1)	**Log Likelihood**	-1338.802
Date:	Sun, May 04 2025	**AIC**	2681.604
Time:	14:49:14	**BIC**	2688.951
Sample:	01-01-2001 - 05-01-2025	**HQIC**	2684.547
Covariance Type:	opg		

	coef	std err	z	P> |z|	[0.025	0.975]
ma.L1	-0.9816	0.018	-54.597	0.000	-1.017	-0.946
sigma2	573.8893	41.967	13.675	0.000	491.636	656.143

Ljung-Box (L1) (Q):	0.00	**Jarque-Bera (JB):**	26.11
Prob(Q):	0.94	**Prob(JB):**	0.00
Heteroskedasticity (H):	1.06	**Skew:**	-0.47
Prob(H) (two-sided):	0.79	**Kurtosis:**	4.13

A.3 t-GARCH

A.3.1 Interest Rate

Dep. Variable:	CPI	**R-squared:**	0.000
Mean Model:	Zero Mean	**Adj. R-squared:**	0.004
Vol Model:	GARCH	**Log-Likelihood:**	-143.658
Distribution:	Standardized Student's t	**AIC:**	299.316
Method:	Maximum Likelihood	**BIC:**	321.017
		No. Observations:	275
Date:	Sun, May 04 2025	**Df Residuals:**	275
Time:	21:29:04	**Df Model:**	0

	coef	**std err**	**t**	**P> |t|**	**95.0% Conf. Int.**
omega	0.0236	1.119e-02	2.110	3.483e-02	[1.683e-03,4.557e-02]
alpha[1]	0.0169	3.115e-02	0.541	0.588	[-4.419e-02,7.792e-02]
alpha[2]	0.1525	7.544e-02	2.022	4.320e-02	[4.666e-03, 0.300]
beta[1]	1.0453e-13	0.126	8.282e-13	1.000	[-0.247, 0.247]
beta[2]	0.7151	0.206	3.475	5.114e-04	[0.312, 1.118]
	coef	**std err**	**t**	**P> |t|**	**95.0% Conf. Int.**
nu	5.3048	1.754	3.024	2.498e-03	[1.866, 8.743]

Covariance estimator: robust

A.3.2 Inflation

Dep. Variable:	InterestRate	**R-squared:**	0.000
Mean Model:	Zero Mean	**Adj. R-squared:**	0.004
Vol Model:	GARCH	**Log-Likelihood:**	144.040
Distribution:	Standardized Student's t	**AIC:**	-280.080
Method:	Maximum Likelihood	**BIC:**	-265.613
		No. Observations:	275
Date:	Sun, May 04 2025	**Df Residuals:**	275
Time:	22:24:32	**Df Model:**	0

	coef	**std err**	**t**	**P> |t|**	**95.0% Conf. Int.**
omega	7.4467e-03	3.889e-03	1.915	5.550e-02	[-1.752e-04,1.507e-02]
alpha[1]	0.0452	5.220e-02	0.866	0.386	[-5.709e-02, 0.148]
beta[1]	0.5982	0.205	2.919	3.509e-03	[0.197, 1.000]
	coef	**std err**	**t**	**P> |t|**	**95.0% Conf. Int.**
nu	13.6250	9.589	1.421	0.155	[-5.169, 32.419]

Covariance estimator: robust

A.3.3 AEX

Dep. Variable:	None	**R-squared:**	0.000
Mean Model:	Constant Mean	**Adj. R-squared:**	0.000
Vol Model:	GARCH	**Log-Likelihood:**	-1337.65
Distribution:	Standardized Student's t	**AIC:**	2685.29
Method:	Maximum Likelihood	**BIC:**	2703.69
		No. Observations:	293
Date:	Fri, Jun 13 2025	**Df Residuals:**	292
Time:	14:49:14	**Df Model:**	1

	coef	std err	t	P> |t|	95.0% Conf. Int.
mu	4.7088	1.130	4.166	3.103e-05	[2.493, 6.924]
	coef	**std err**	**t**	**P> |t|**	**95.0% Conf. Int.**
omega	83.6303	50.814	1.646	9.980e-02	[-15.962,1.832e+02]
alpha[1]	0.2579	9.292e-02	2.775	5.515e-03	[7.576e-02, 0.440]
beta[1]	0.6016	0.131	4.603	4.163e-06	[0.345, 0.858]
	coef	**std err**	**t**	**P> |t|**	**95.0% Conf. Int.**
nu	6.7723	2.108	3.212	1.316e-03	[2.640, 10.904]

Covariance estimator: robust

A.4 Nominal Stability ($\mu = 0$)

Age	mean25	var25	mean500	var500	mean3000	var3000
67	8117	0	8117	0	8117	0
68	8133	33407	8133	1584	8133	266
69	8143	75703	8138	3178	8138	553
70	8101	118194	8089	5171	8086	865
71	8088	175828	8063	7056	8061	1203
72	8165	239640	8135	9368	8133	1673
73	8201	298752	8174	12461	8171	2162
74	8194	367390	8156	15644	8152	2559
75	8224	468485	8173	19034	8169	3155
76	8248	555343	8194	23094	8189	3875
77	8285	675129	8208	28373	8201	4771
78	8281	831070	8195	34464	8188	5529
79	8341	990093	8220	40715	8215	6508
80	8348	1227159	8181	49154	8175	7663
81	8381	1429516	8189	57788	8184	9306
82	8428	1694800	8220	70496	8213	10884
83	8470	1976045	8246	86324	8234	12748
84	8551	2384404	8298	103295	8281	15118
85	8648	3267822	8318	120776	8301	18112
86	8683	4206904	8295	145839	8272	20979
87	8803	5955743	8320	177617	8287	26313
88	8957	7773665	8373	226123	8336	33051
89	9225	10578275	8430	279069	8388	42658
90	9584	17437566	8498	364865	8448	56437
91	10061	31353335	8460	461079	8403	73168
92	10406	44414585	8482	630000	8409	99690
93	10647	49906733	8469	853910	8383	128760
94	10165	44941852	8486	1157892	8390	178864
95	9082	36319534	8478	1511568	8362	232862
96	7216	25600316	8527	2159288	8344	334187
97	5007	16078070	8681	3420539	8405	513131
98	3004	8813690	8981	6927423	8489	826279
99	1527	3706705	9438	20115680	8517	1440491
100	698	1278360	10180	43281496	8587	2442760
101	273	339735	10608	51756836	8722	4247219
102	95	73780	8478	34255224	9121	11407975
103	28	12767	4757	16367313	9897	33568119
104	8	1901	1933	5348261	10662	51407573
105	2	232	595	1108739	7826	29612389
106	0	25	145	153678	3334	10580406
107	0	3	31	16680	977	2210416
108	0	0	6	1546	233	295755
109	0	0	1	154	46	28191

A.5 Real Stability Distribution ($\mu = 0.2$)

	Bootstrapped Percentile										
	0%	**10%**	**20%**	**30%**	**40%**	**50%**	**60%**	**70%**	**80%**	**90%**	**100%**
Age											
67	8117	8117	8117	8117	8117	8117	8117	8117	8117	8117	8117
68	7999	8032	8037	8042	8047	8050	8056	8061	8067	8072	8105
69	7833	7875	7887	7892	7899	7905	7911	7916	7925	7932	7971
70	7917	7964	7977	7985	7994	7999	8007	8016	8027	8038	8126
71	7678	7742	7756	7766	7777	7783	7791	7802	7812	7829	7908
72	7521	7590	7609	7620	7628	7639	7648	7659	7672	7688	7772
73	7741	7814	7834	7848	7859	7871	7879	7891	7908	7928	8056
74	7726	7797	7818	7835	7846	7859	7870	7885	7900	7923	8041
75	7846	7935	7959	7974	7992	8004	8017	8035	8054	8078	8186
76	7780	7872	7899	7918	7932	7948	7964	7979	7999	8027	8143
77	7641	7792	7816	7835	7854	7870	7889	7908	7931	7960	8099
78	7629	7774	7803	7826	7845	7862	7881	7901	7928	7958	8119
79	7490	7606	7635	7661	7681	7701	7721	7741	7765	7799	7967
80	7429	7572	7605	7633	7653	7671	7695	7719	7745	7787	7936
81	7214	7355	7393	7417	7442	7466	7488	7513	7541	7585	7760
82	7102	7258	7294	7323	7348	7370	7400	7426	7456	7497	7736
83	6989	7178	7219	7249	7276	7300	7330	7358	7390	7433	7639
84	6806	7006	7057	7092	7117	7145	7169	7202	7235	7285	7519
85	6683	6918	6973	7010	7041	7066	7092	7127	7162	7216	7516
86	6563	6785	6844	6880	6912	6940	6968	7005	7043	7096	7495
87	6502	6709	6768	6817	6848	6883	6914	6950	6992	7056	7428
88	6372	6733	6800	6845	6885	6919	6959	6995	7042	7115	7514
89	6330	6707	6783	6834	6879	6919	6959	7007	7061	7145	7744
90	6188	6551	6637	6696	6748	6801	6847	6894	6957	7047	7483
91	5994	6414	6507	6567	6629	6682	6737	6793	6868	6965	7481
92	5874	6348	6451	6524	6588	6654	6710	6789	6871	6979	7645
93	5770	6353	6480	6573	6628	6711	6782	6854	6958	7096	7956
94	5606	6264	6411	6513	6600	6691	6764	6840	6956	7138	7947
95	5541	6098	6245	6354	6467	6561	6657	6756	6884	7071	8261
96	5195	5931	6098	6245	6336	6462	6593	6730	6872	7098	8435
97	4901	5750	5980	6101	6272	6406	6547	6693	6847	7118	9343
98	4777	5625	5844	6019	6206	6336	6543	6763	6919	7252	10203
99	4217	5330	5644	5815	6091	6190	6504	6732	6978	7380	11993
100	4172	5061	5406	5663	5946	6099	6428	6795	7207	7672	13215
101	3357	4588	5097	5294	5734	5984	6256	6554	7244	8096	15294
102	3106	4314	4568	4854	5547	5547	5974	6472	7060	8629	38834
103	2364	3545	4254	4727	5318	5318	6078	6079	7091	8510	42553
104	1708	3173	3702	4442	4442	5552	5553	7404	7404	11107	22218
105	1387	2775	2776	3701	3702	3702	5552	5553	5553	11105	11107
106	883	1766	1767	2650	2650	2650	5299	5299	5300	5300	5301
107	613	1227	1227	1228	2455	2455	2455	2455	2455	2455	2455
108	363	545	1090	1090	1090	1090	1090	1090	1090	1090	1090
109	234	467	467	467	467	467	468	468	468	468	468

A.6 Real Stability Distribution with Backloading ($\mu = 0.2$)

	Bootstrapped Percentile										
	0%	**10%**	**20%**	**30%**	**40%**	**50%**	**60%**	**70%**	**80%**	**90%**	**100%**
Age											
67	7306	7306	7306	7306	7306	7306	7306	7306	7306	7306	7306
68	7245	7267	7274	7277	7282	7284	7288	7293	7298	7303	7329
69	7205	7245	7254	7262	7267	7272	7277	7282	7290	7299	7329
70	7381	7427	7438	7445	7453	7460	7466	7474	7484	7494	7576
71	7233	7294	7309	7317	7328	7335	7342	7351	7361	7377	7450
72	7105	7174	7191	7199	7209	7217	7228	7235	7248	7264	7327
73	7389	7455	7478	7491	7499	7510	7518	7530	7546	7568	7630
74	7460	7531	7551	7565	7576	7587	7601	7613	7627	7647	7765
75	7675	7762	7785	7801	7818	7831	7843	7857	7876	7903	8007
76	7664	7756	7777	7798	7813	7828	7841	7859	7878	7909	8011
77	7682	7808	7829	7851	7867	7883	7902	7918	7944	7973	8105
78	7752	7889	7919	7942	7962	7982	7998	8019	8046	8080	8240
79	7704	7822	7852	7879	7900	7921	7941	7962	7990	8025	8194
80	7743	7888	7927	7952	7973	7998	8020	8045	8072	8116	8271
81	7620	7770	7809	7832	7857	7884	7910	7940	7974	8016	8197
82	7603	7737	7783	7814	7841	7864	7896	7927	7956	8004	8183
83	7553	7719	7759	7791	7820	7849	7883	7912	7950	7993	8215
84	7312	7527	7582	7620	7646	7676	7703	7738	7778	7823	8055
85	7237	7431	7494	7535	7562	7594	7622	7655	7703	7761	7954
86	7119	7282	7354	7393	7422	7457	7487	7522	7558	7615	7839
87	7003	7196	7269	7317	7349	7382	7421	7459	7505	7567	7829
88	6989	7250	7327	7375	7412	7449	7487	7525	7589	7661	7947
89	6855	7110	7197	7251	7294	7335	7378	7428	7486	7575	7912
90	6528	6917	7000	7063	7126	7174	7223	7273	7339	7434	7826
91	6295	6745	6833	6898	6962	7028	7086	7144	7214	7326	7857
92	6084	6566	6682	6770	6825	6893	6951	7021	7106	7242	7919
93	5994	6587	6733	6802	6858	6944	7017	7107	7215	7358	8250
94	5756	6431	6583	6688	6778	6851	6927	7023	7143	7330	8159
95	5665	6219	6347	6435	6526	6644	6741	6841	6970	7187	8396
96	5246	5989	6158	6306	6430	6525	6625	6761	6940	7129	8518
97	4977	5807	6039	6204	6335	6470	6565	6760	6915	7190	9437
98	4928	5619	5838	6012	6198	6330	6535	6755	6911	7244	9857
99	4570	5407	5645	5817	6093	6293	6507	6735	6980	7383	10103
100	4129	5117	5350	5605	5885	6036	6362	6725	7133	7594	11771
101	3276	4632	4975	5168	5597	5841	6106	6398	7071	7902	13436
102	3011	4182	4428	5018	5376	5790	5791	6273	6844	8364	37644
103	2262	3394	4072	4525	5091	5091	5819	6787	6789	8147	40735
104	1617	3004	3505	4206	4206	5257	5258	5258	7010	10516	21035
105	1299	2598	2599	3465	3465	3465	5198	5198	5198	10396	10398
106	815	1631	1631	2447	2447	2447	4893	4894	4894	4894	4894
107	557	1113	1114	1114	2227	2227	2227	2227	2227	2227	2228
108	321	482	482	965	965	965	965	965	965	965	965
109	198	198	397	397	397	397	397	397	397	397	397

B Figures

Backloading Paths with $\mu = 0.3$

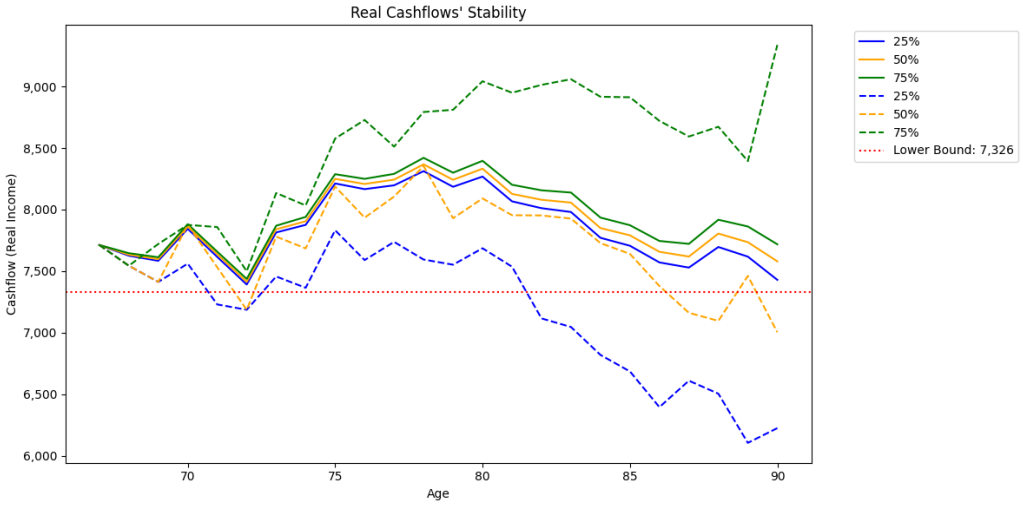

Figure 11: Plots of the paths of the 25th, 50th and 75th percentiles of real cash-flows from age of inception to age 90 for variable $n = 25, 100$ number of constituents in comparison to the threshold (3.26) at which cash-flow stability is set and fixed equity allocation of investments of $\mu = 30\%$ with arbitrary backloading (3.10).